Original Article

Improvements in left ventricular regional and global systolic function following treatment with S100A4-shRNA after myocardial infarction in mice

Lijun Qian[1#], Yanjuan Zhang[2#], Menglin Zhu[1], Feng Xie[3], Thomas R. Porter[3], Di Xu[1]

[1]Department of Geriatrics, [2]Department of Cardiology, The First Affiliated Hospital of Nanjing Medical University, Nanjing 210029, China; [3]Department of Internal Medicine, University of Nebraska Medical Center, Omaha, Nebraska 68198, USA

[#]These authors contributed equally to this work.

Correspondence to: Di Xu, MD, PhD. Department of Geriatrics, The First Affiliated Hospital of Nanjing Medical University, 140 Hanzhong Road, Nanjing 210029, China. Email: xudi@jsph.org.cn; Thomas R. Porter, MD. University of Nebraska Medical Center, Omaha, NE 68198, USA. Email: trporter@unmc.edu.

Background: S100A4 plays a vital role in cardiac fibrosis after myocardial infarction (MI), but its effects on myocardial mechanics and remodeling are unknown. We hypothesized that regional and global left ventricular (LV) systolic function as determined by speckle tracking echocardiography (STE) would be improved with inhibition of S100A4 using short hairpin (sh) RNA. This study aimed to investigate whether STE can delineate the efficacy and safety of S100A4-shRNA in MI.

Methods: A total of 48 mice were randomly assigned to sham+S100A4-shRNA, sham+scrambled (Scr) sequence-shRNA, MI+S100A4-shRNA, and MI+Scr-shRNA groups (n=12 per group) and underwent intramyocardial injection of target agents after MI was produced by left anterior descending ligation. Two-dimensional STE and M-mode echocardiography were performed at baseline and at day 7, 14, and 28 post-MI by GE Vivid 7 ultrasound (il3L linear probe, 10.0–14.0 MHz) and Echopac PC software. Radial strain was analyzed from 6 segments of the mid short axis images with 20–30 frames per cardiac cycle. Post-mortem western blotting, immunohistochemistry, and Masson's trichrome stain were performed to quantify infarct size and detect suppression of S100A4.

Results: STE detected a statistically significant improvement in peak radial strain (pRS) and time to peak radial strain (pRSt) by day 14 post-MI in the MI+S100A4-shRNA group ($P<0.05$), especially in the LV anteroseptal wall (pRS: 23.83%±1.12% *vs.* 20.25%±1.02%, pRSt: 76.75±3.18 *vs.* 92.00±3.69 ms, $P<0.05$). After 1 month of S100A4-shRNA administration, cardiac function improved in the MI+S100A4-shRNA group according to both STE and M-mode tracing in mice. Additionally, both biochemical and histopathological examinations found reduced cardiac fibrosis in the MI+S100A4-shRNA group.

Conclusions: S100A4-shRNA can be utilized as a therapeutic target to improve regional deformation and attenuate cardiac fibrosis following MI. Two-dimensional STE is useful in the early and comprehensive assessment of LV systolic function in mice.

Keywords: S100A4; strain analysis; cardiac fibrosis; myocardial infarction (MI)

Submitted Nov 29, 2018. Accepted for publication May 23, 2019.
doi: 10.21037/qims.2019.05.25
View this article at: http://dx.doi.org/10.21037/qims.2019.05.25

© Quantitative Imaging in Medicine and Surgery. All rights reserved.

Introduction

Myocardial infarction (MI) is a leading cause of death worldwide (1). Although statins, anticoagulants (2), and percutaneous coronary intervention are widely used (3), heart failure still occurs after various kinds of adverse cardiac remodeling post-MI (4). Cardiac fibrosis plays an important role in cardiac remodeling, leading to left ventricular (LV) systolic and diastolic dysfunction (5). However, effective diagnose and therapy for cardiac fibrosis remain undeveloped.

Echocardiography is a diagnostic method that can meet both clinical and basic medical needs because of its non-invasive, cost-effective, and time-saving nature (6). However, its occasional imprecise evaluation of disease severity and prognosis has necessitated its reformation (7). Recently, a novel technique named two-dimensional speckle tracking echocardiography (STE) has matured (8) with the ability to dramatically improve the accuracy in assessing cardiac performance based on myocardial strain analysis (9). Strain analysis provides integrated and detailed information with much higher sensitivity and specificity by capturing segmental tissue motions on multiple planes and axes (10).

S100 calcium-binding A4 (S100A4), also known as fibroblast-specific protein 1 (Fsp1), is unregulated in fibrotic diseases of the lung (11), liver (12), kidney (13) and heart (14). Coming from the S100 gene family (15), it is involved in immune response, differentiation, cytoskeleton dynamics, and cell growth (16). Our previous study has found that downregulation of S100A4 alleviates cardiac fibrosis via Wnt/β-catenin pathway in mice, which may provide a potential therapeutic target for cardiac fibrosis after MI (17). However, more animal experiments, safety assessments, and efficient myocardial transfections are needed to enhance our findings.

In this study, we investigated the role of two-dimensional STE in the early assessment of myocardial function after MI, detected the potential parameters of stain analysis, and verified the efficacy and safety of S100A4-shRNAin cardiac fibrosis in murine MI model.

Methods

Animal and ethics

All experiments were approved by the Live Animals Committee in Teaching and Research at Nanjing Medical University (Approval ID: IACUC-1703039). The study was performed in accordance with the guidelines and principles for the care and use of laboratory animals published by the National Institutes of Health (No. 85-23, revised 1996).

C57BL/6 mice (6 weeks old) weighing 20–25 g was obtained from Nanjing University Model Animal Research Center. They were kept in a 12 h/12 h light/dark cycle at a room temperature for least 10 days and fed with a standard diet before the experiment. Baseline vital signs and myocardial function were recorded.

Study protocol

A total of 48 male mice were randomly assigned to sham+S100A4-shRNA, sham+scrambled (Scr) sequence-shRNA, MI+S100A4-shRNA, and MI+Scr-shRNA groups (n=12 per group) by controlling two independent variables (MI and S100A4-shRNA administration). To detect LV regional and global systolic changes, we assessed cardiac function via both M-mode tracing and strain analysis at baseline, day 7, 14, and 28 after injection. Then, mice were sacrificed for further histolytic study at the 28th day post echocardiography.

Surgery and gene transfection

Mice were anesthetized with 0.5% sodium pentobarbital (100 mg/kg) and then intubated and ventilated at 120 bpm during the operation. In the MI groups, the left anterior descending (LAD) coronary artery was ligated at 2 mm from the tip of the left auricle with 7–0 silk suture. After that, MI was confirmed by S-T segment elevation on an electrocardiogram. A volume of 5×10^5 pfu/g Scr-shRNA or S100A4-shRNA was intramyocardially injected into 5 parts bordering the infarction zone or normal region via a 30-gauge Hamilton needle. The sham groups underwent chest open operation but no LAD ligation, and received the same dose and positions of Scr-shRNA or S100A4-shRNA administration shortly after the surgical procedure. The optimal transfection concentration (2.5 μL/g, 2×10^7 pfu/mL) was determined by GFP expression rate and cell viability.

M-mode echocardiography

A Vivid 7 ultrasound (GE, Horten, Norway) equipped with an il3L intraoperative linear probe at 10.0–14.0 MHz was used in the study. The mice were imaged under light sedation and decreasing ambient lighting at 22–24 ℃ by an experienced handler. M-mode parameters were obtained at the mid-papillary level in the short-axis parasternal

© Quantitative Imaging in Medicine and Surgery. All rights reserved.

view, including inter ventricular septal diameter (IVSd), left ventricular posterior wall thickness (LVPWd), left ventricular internal diameter at diastole (LVIDd), left ventricular internal diameter at systole (LVIDs), ejection fraction (EF), and fractional shortening (FS).

Strain analysis

Circumferential and radial strain were analyzed from 3 consecutive cardiac cycles of the mid-LV (parasternal papillary muscle level) short axis images by Echopac PC software (version 113.1, GE, Horten, Norway). Region of interest was measured by manually contouring the area between endocardial and epicardia borders. Grayscale images were then analyzed following frame-to-frame movement of stable patterns of natural acoustic markers (or speckles) over each cardiac cycle with frame rates ranging from 200 to 300 fps. Finally, the values of peak radial strain (pRS) and time to peak radial strain (pRSt) were derived from 6 segments by strain analysis.

Masson trichrome staining

The LV tissues were fixed in 4% buffered formalin, embedded in paraffin, and then prepared into 5-μm-thick sections. Masson staining was performed to investigate the distribution and assess the extent of myocardial interstitial fibrosis.

Immunohistochemistry (IHC)

The tissues were prepared into 5-μm-thick paraffin sections with deparaffinization and antigen retrieval in 1 mM EDTA (pH 9.0) for 15 min. Then, slides were applied with 5% bovine serum albumin (BSA) at room temperature for 1 h, and incubated with primary antibodies at 4 ℃ overnight and secondary antibodies at room temperature for 30 min. Before mounting, chromogens (diaminobenzidine or 3-amino-9-ethylcarbazole) and hematoxylin were used for counterstain.

Statistical analysis

All experiments were repeated and obtained with repetitions of qualitatively similar data. All data were analyzed by SPSS 17.0 (Chicago, IL, USA) and GraphPad Prism 6.0 software (CA, USA). Intergroup comparison of the continuous numerical variables was tested by *t*-test or two-way ANOVA. Values were expressed as mean ± standard deviation, and $P<0.05$ was considered statistically significant.

Results

Basic characteristics

A total of 48 male mice were randomly assigned to study groups and treatment regimes. There was no significant difference in the vital baseline signs and cardiac function between the sham+Scr-shRNA, sham+S100A4-shRNA, MI+Scr-shRNA, and MI+S100A4-shRNA groups (all $P>0.05$) (*Table 1*).

M-mode echocardiography detected LV deformation after MI

We discovered significant change in the LV deformation before and at day 7 and 28 post-MI (all n=24) (*Figure 1A*). M-mode tracings showed the values of EF (77.83%±3.24% *vs.* 37.33%±3.50%, $P<0.05$) and FS (40.33%±2.43% *vs.* 18.50%±0.96%, $P<0.05$) statistically decreased at the 7th day compared with the baseline group. After that, EF (44.17%±2.67% *vs.* 37.33%±3.50%, $P<0.05$) increased on the 28th day, compared with the 14th day tracings (*Figure 1B*). In addition, compared with day 14, FS (22.33%±2.43% *vs.* 18.50%±0.96%, $P<0.05$) significantly increased on day 28 (*Figure 1C*). M-mode imaging showed cardiac function dropped after MI and improved after 1-month repatriation.

Early identification by STE of cardiac changes in pRS and pRSt post-MI

To detect the changes of LV regional systolic function after MI, radial strain analysis was performed via two-dimensional STE (all n=24, *Table 2*). Examples showed a significant increase of LV systolic function in the 14th day compared with the day 7 group (*Figure 2A*). A marked increase of pRS (anteroseptal, 23.83%±1.12% *vs.* 20.25%±1.02%, $P<0.05$; anterior, 23.17%±1.03% *vs.* 20.08%±1.08%, $P<0.05$; inferoseptal, 22.92%±1.15% *vs.* 19.58%±1.03%, $P<0.05$) was detected between the 7th and 14th day, especially in the LV anteroseptal wall (*Figure 2B*). Additionally, pRSt statistically decreased (anteroseptal 76.75±3.18 *vs.* 92.00±3.69 ms, $P<0.05$; anterior, 76.92±2.64 *vs.* 91.42±2.52 ms, $P<0.05$; inferoseptal, 74.58±2.60 *vs.* 88.42±2.09 ms, $P<0.05$) in the day 14 group compared with

© Quantitative Imaging in Medicine and Surgery. All rights reserved.

Table 1 Baseline characteristics of study animals

Parameters	Sham+Scr-shRNA (n=12)	Sham+S100A4-shRNA (n=12)	MI+Scr-shRNA (n=12)	MI+S100A4-shRNA (n=12)	P value
Weight (g)	22.30±2.67	23.60±3.13	22.90±2.73	23.20±3.41	0.75
HR (bpm)	557.8±12.23	554.6±14.34	551.8±13.62	553.4±14.34	0.74
Temperature (℃)	37.19±2.23	37.83±2.18	38.19±1.52	37.72±1.88	0.67
Breath (bpm)	160.87±10.54	165.72±11.34	160.87±9.54	169.72±12.34	0.16
IVSd (mm)	0.81±0.12	0.83±0.17	0.75±0.13	0.78±0.19	0.61
LVPWd (mm)	0.66±0.16	0.71±0.11	0.70±0.09	0.68±0.13	0.77
LVIDs (mm)	1.53±0.15	1.58±0.21	1.46±0.23	1.61±0.19	0.28
LVIDd (mm)	2.55±0.17	2.53±0.19	2.49±0.24	2.43±0.28	0.58
EF (%)	77.33±3.68	77.50±2.63	78.83±3.24	76.83±4.21	0.55
FS (%)	40.17±5.48	41.68±4.21	39.96±5.07	41.39±4.86	0.78

Values are mean ± SD. BP, blood pressure; HR, heart rate; IVSd, inter ventricular septal diameter; LVPWd, left ventricular posterior wall thickness at diastole; LVIDd, left ventricular internal diameter at diastole; LVIDs, left ventricular internal diameter at systole; EF, ejection fraction; FS, fractional shortening. P values were obtained using two-way ANOVA test.

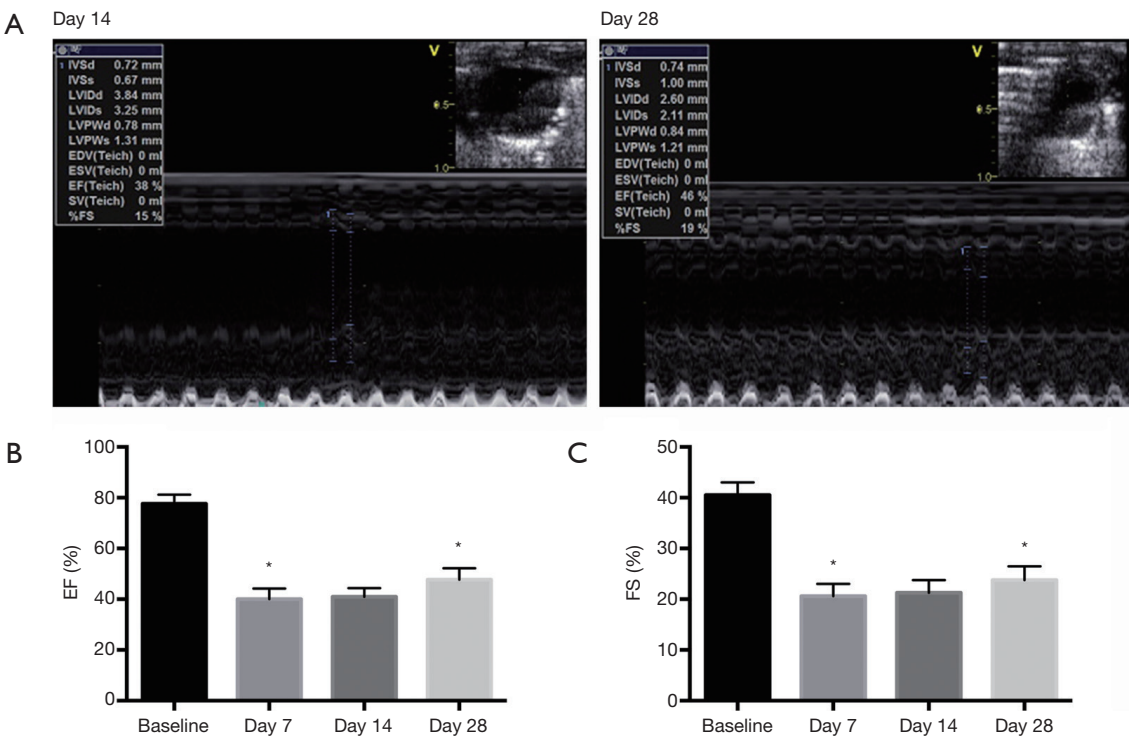

Figure 1 Cardiac function diminution via standard echocardiography. (A) M-mode echocardiography indicated cardiac deformation between the day 14 and day 28 groups. (B) EF values decreased between the 7th *vs.* 0 day group and increased until the 28th day. (C) Compared with the day 14 group, FS values significantly increased in the day 28 group. EF, ejection fraction; FS, fractional shortening; P values were obtained using Student's *t*-test; *, day 7 *vs.* baseline group, P<0.05; day 28 *vs.* day 14 group, P<0.05; n=24 per group.

© Quantitative Imaging in Medicine and Surgery. All rights reserved.

Table 2 Left ventricular systolic function detected after MI by speckle tracking echocardiography

Variable	Baseline (n=24)	Day 7 (n=24)	Day 14 (n=24)	Day 28 (n=24)
Peak radial strain				
Anteroseptal (%)	31.42±1.45	20.25±1.02*	23.83±1.12#	26.83±1.03^
Anterior (%)	31.56±1.64	20.08±1.08*	23.17±1.03#	26.42±0.69^
Inferoseptal (%)	32.17±1.24	19.58±1.03*	22.92±1.15#	26.92±0.65^
Time to peak radial strain				
Anteroseptal (ms)	39.92±2.09	92.00±3.69*	76.75±3.18#	66.67±3.26^
Anterior (ms)	39.83±1.36	91.42±2.52*	76.92±2.64#	68.75±2.31^
Inferoseptal (ms)	40.08±1.22	88.42±2.09*	74.58±2.60#	68.08±2.29

Value are means ± SD. P values were obtained using Student's *t*-test. *, day 7 *vs.* baseline group, P<0.05; #, day 14 *vs.* day 7 group, P<0.05; ^, day 28 *vs.* day 14 group, P<0.05.

the day 7 group (*Figure 2C*). The results revealed that STE identified positive changes of LV systolic function on day 14 post-MI, which is earlier than that in the M-mode tracings.

S100A4-shRNA improves LV systolic function after MI

To detect the efficacy of S100A4-shRNA in attenuating regional deformation among sham+Scr-shRNA, sham+S100A4-shRNA, MI+S100A4-shRNA, and MI+Scr-shRNA groups, M-mode echo and strain analysis were used at the 28th day post-surgery (n=12 per group, *Table 3*). M-mode echo showed both EF (50.50%±0.72% *vs.* 43.42%±0.82%, P<0.05) (*Figure 3A*) and FS (27.42%±0.71% *vs.* 21.92%±0.77%, P<0.05) (*Figure 3B*) increased in the MI+S100A4-shRNA group, compared with the MI+Scr-shRNA group. STE showed significant elevation of pRS (29.00%±0.87% *vs.* 24.67%±0.71%, P<0.05) in the anteroseptal segment (*Figure 3C*), and a decline of pRSt (60.67±1.43 *vs.* 73.42±3.54 ms, P<0.05) in the LV anteroseptal wall (*Figure 3D*) in the MI+S100A4-shRNA group, compared with the MI+Scr-shRNA group. The results demonstrated that S100A4-shRNA was effective in alleviating LV systolic function after MI.

S100A4-shRNA alleviated cardiac fibrosis after MI

Western blotting showed the expression of α-SMA (*Figure 4A,B*), collagen I (*Figure 4A,C*) protein decrease (fibrosis markers), and S100A4 level decline (*Figure 4A,D*) in the MI+S100A4-shRNA group, compared with the MI+Scr-shRNA group. The extent of cardiac fibrosis reduced in the MI+S100A4-shRNA group (18.91%±2.38% *vs.* 32.39%±3.06%, P<0.05) according to representative Masson's trichrome staining (*Figure 4E*). Immunohistochemistry showed that the levels of α-SMA decreased in the MI+S100A4-shRNA group (15.80%±1.49% *vs.* 27.13%±2.41%, P<0.05) (*Figure 4F*). The results revealed the role of S100A4-shRNA in attenuating cardiac fibrosis after MI.

Discussion

We investigated the role of two-dimensional STE in early and comprehensive assessment of regional LV function after MI, and assessed the efficacy and safety of S100A4-shRNA in cardiac fibrosis after MI in mice. Firstly, M-mode imaging verified LV systolic function significantly declined after MI, and then improved 1 month later (*Figure 1*). Secondly, STE was more effective in the early assessment of cardiac deformation on the 14th day post-MI compared with conventional echocardiography (*Table 2*, *Figure 2*). Furthermore, LV global and regional systolic function statistically improved in the MI+S100A4-shRNA group by M-mode echo and strain analysis (*Table 3*, *Figure 3*). In addition, western blotting, Masson's trichrome staining, and immunohistochemistry showed the efficacy of S100A4-shRNA in attenuating cardiac fibrosis after MI (*Figure 4*).

In the study, we qualified two new parameters for radial strain-based analysis: pRS and pRSt. They could reliably detect cardiac dysfunction in the LV anteroseptal, anterior, and inferoseptal walls after LAD coronary artery ligation. STE is a novel technology for analyzing motion and has abundant indicators (18), even though some of these indicators from strain analysis are considered useless in analyzing the small heart of target animals (19). Studies

© Quantitative Imaging in Medicine and Surgery. All rights reserved.

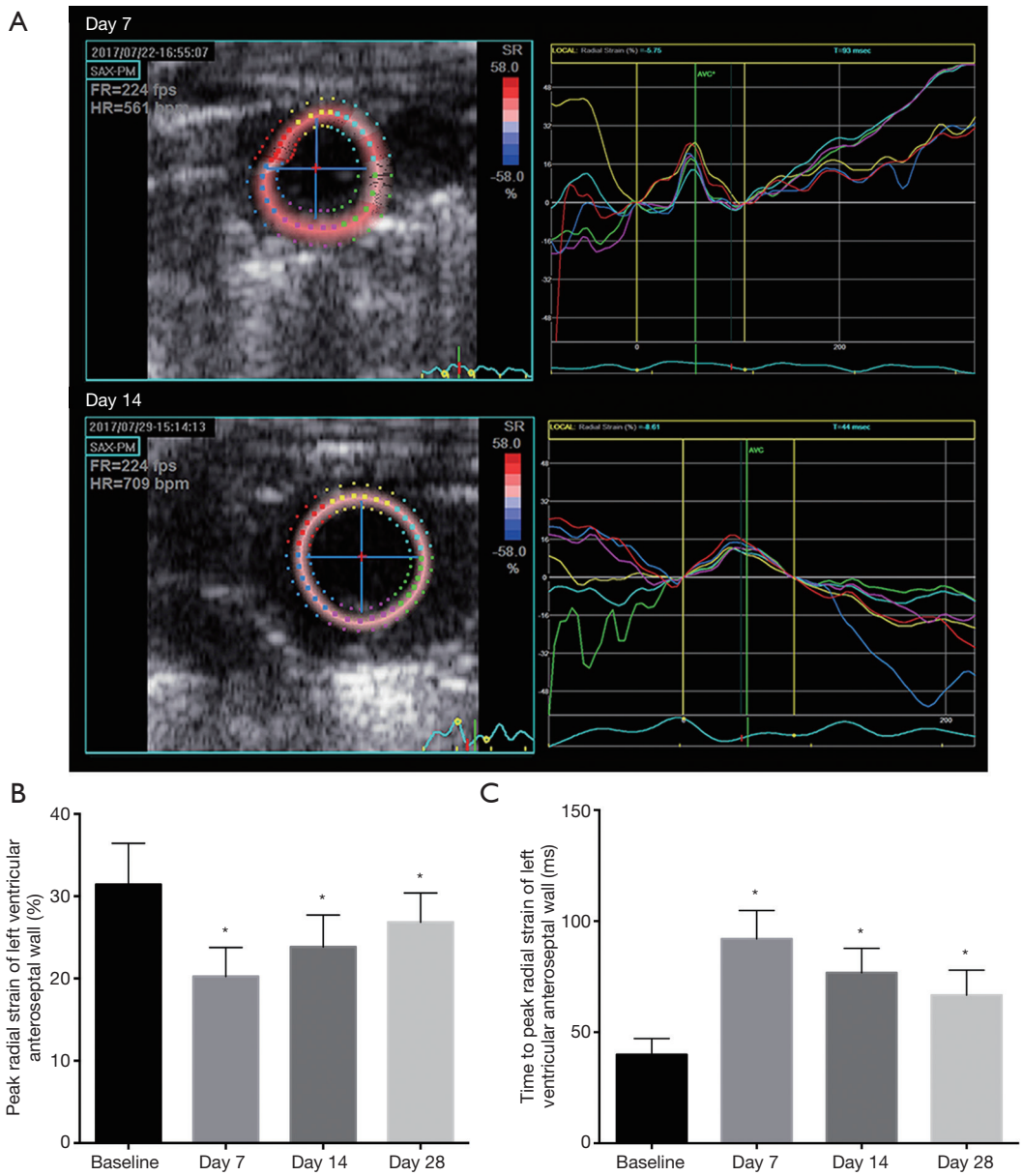

Figure 2 Earlier identification by STE of cardiac remolding after MI. (A) Examples of left ventricular myocardial function assessments as shown by strain analysis at day 7 and day 14; (B) marked increase of peak radial strain indicated by STE between the 14th and 7th day groups; (C) time to peak radial strain decreased in anteroseptal wall in the day 14 group, compared with the day 7 group. P values were obtained using Student's *t*-test; *, day 7 *vs.* baseline group, P<0.05; day 14 *vs.* day 7 group, P<0.05; day 28 *vs.* day 14 group, P<0.05; n=24 per group. STE, speckle tracking echocardiography; MI, myocardial infarction.

have proven circumferential strain to be highly sensitive in detecting cardiac function in mice (20); however, a comprehensive evaluating system for STE has not been conducted yet. Thus, our findings will be beneficial in constructing a new STE assessment system.

Previous research commonly used clinical echocardiography (with frequencies of up to 15 MHz) and simple parameters, like LV size (21). Therefore, the statistical data on circumferential and longitudinal strain in our study were not analyzed because of the low ultrasound frequency and image quality. However, studies with high frequency transducers (30 MHz) have shown their reliability and reproducibility

© Quantitative Imaging in Medicine and Surgery. All rights reserved.

Table 3 Left ventricular global and regional systolic function detected at day 28 post-surgery

Variable	sham+Scr-shRNA (n=12)	sham+S100A4-shRNA (n=12)	MI+Scr-shRNA (n=12)	MI+S100A4-shRNA (n=12)
EF (%)	77.08±1.38	75.75±1.16	43.42±0.82*	50.50±0.72#
FS (%)	41.50±1.08	40.67±0.73	21.92±0.77*	27.42±0.71#
Peak radial strain (%)	30.92±1.10	31.67±1.20	24.67±0.71*	29.00±0.87#
Time to peak radial strain (ms)	39.58±2.54	40.50±1.41	73.42±3.54*	60.67±1.43#

Values are mean ± SD. MI, myocardial infarction. P values were obtained using Student's *t*-test or two-way ANOVA. *, MI+Scr-shRNA *vs.* sham+Scr-shRNA group, P<0.05; #, MI+S100A4-shRNA *vs.* MI+Scr-shRNA group, P<0.05.

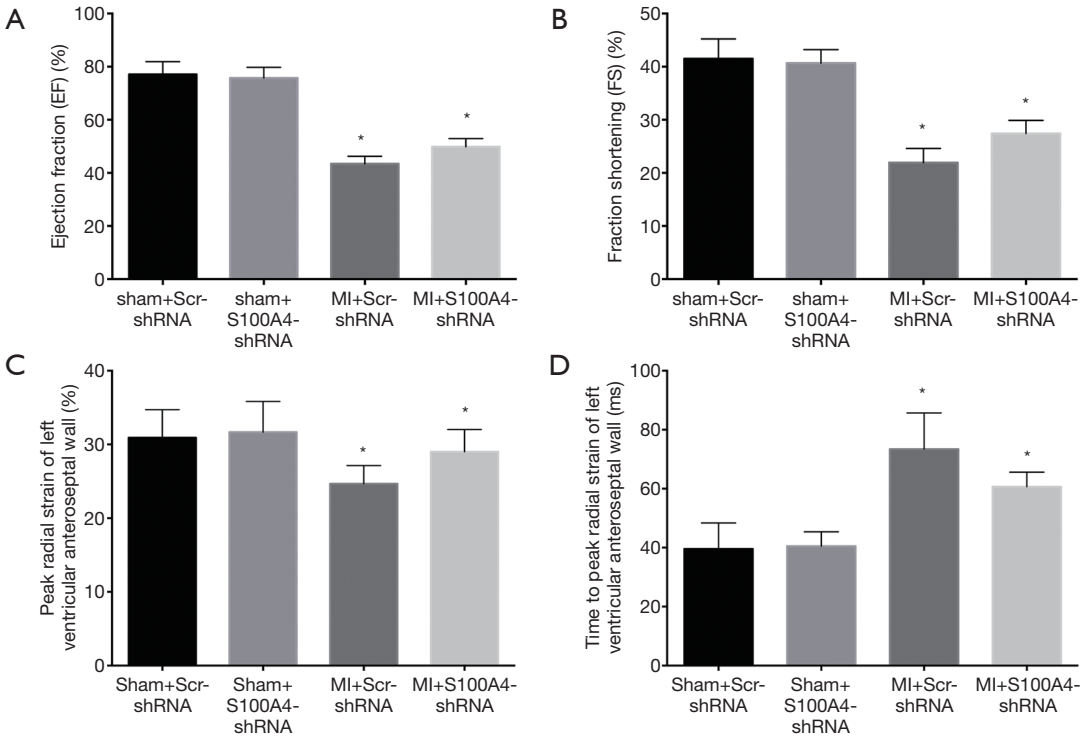

Figure 3 STE and M-mode echo detected the efficacy of S100A4-shRNA in cardiac fibrosis. (A) M-mode echo showed EF increased in the MI+S100A4-shRNA group, compared with the MI+Scr-shRNA group. (B) FS was elevated in the MI+S100A4-shRNA group, compared with the MI+Scr-shRNA group. (C) STE showed significant elevation of radial strain in the MI+S100A4-shRNA group. (D) Time to peak radial strain declined in the MI+S100A4-shRNA group compared with the MI+Scr-shRNA group. P values were obtained using Student's *t*-test or two-way ANOVA. *, MI+S100A4-shRNA *vs.* MI+Scr-shRNA group, P<0.05; MI+Scr-shRNA group *vs.* sham+Scr-shRNA group, P<0.05; n=12 per group. STE, speckle tracking echocardiography; MI, myocardial infarction.

in assessing both global and regional function in the post-MI remodeling of mouse hearts (22-24). Further studies are needed to assess the feasibility and accuracy of high-frequency two-dimensional echocardiography.

Our previous experiments have found that S100A4-shRNA significantly inhibits cardiac fibroblasts differentiation after MI (25). This study provides more evidence of S100A4-shRNA in attenuating myocardial dysfunction and cardiac fibrosis after MI. Nevertheless, the pathophysiology underlying this attenuation and the association between LV remodeling and cardiomyocyte apoptosis remain to be determined. Moreover, with the development of ultrasound targeted microbubble destruction (26), more efforts should be taken to transfect

© Quantitative Imaging in Medicine and Surgery. All rights reserved.

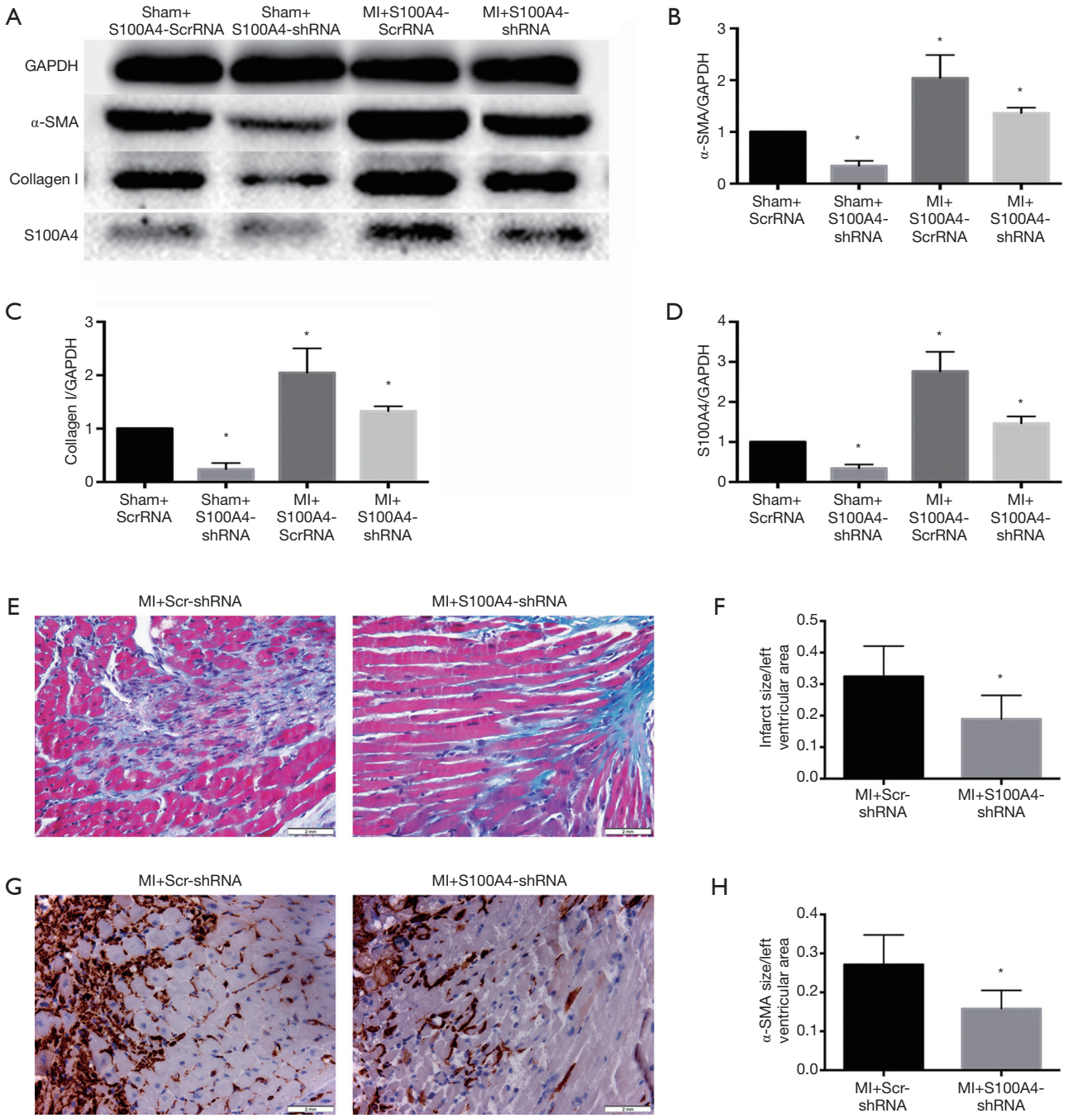

Figure 4 S100A4-shRNA ameliorated cardiac fibrosis after MI. (A,B) Western blotting showed the expression of α-SMA decreased in the MI+S100A4-shRNA group compared with the MI+Scr-shRNA group. (A,C) The expression of collagen I reduced in the MI+S100A4-shRNA group as indicated by western blotting. (A,D) Western blotting showed the S100A4 level declined in the MI+S100A4-shRNA group. (E) Masson's trichrome staining showed that the extent of cardiac fibrosis decreased in the MI+S100A4-shRNA group. (F) Immunohistochemistry showed the levels of α-SMA decreased in the MI+S100A4-shRNA group. P values were obtained using Student's *t*-test or two-way ANOVA. *, MI+S100A4-shRNA *vs.* MI+Scr-shRNA group, P<0.05; MI+Scr-shRNA group *vs.* sham+Scr-shRNA group, P<0.05; sham+S100A4-shRNA group *vs.* sham+Scr-shRNA group, P<0.05; n=12 per group. MI, myocardial infarction.

© Quantitative Imaging in Medicine and Surgery. All rights reserved.

target agents more efficiently and noninvasively.

Conclusions

S100A4-shRNA can be utilized as a therapeutic target to improve regional deformation and attenuate cardiac fibrosis following MI. Two-dimensional STE is useful in the early and comprehensive assessment of LV systolic function in mice.

Acknowledgments

Funding: This study was supported by the National Natural Science Foundation of China (Grant No. 81871359), by Jiangsu Provincial Key Discipline of Medicine (ZDXKA2016003), by the Natural Science Foundation of Jiangsu Province (BK20161057), by the Priority Academic Program Development of Jiangsu Higher Education Institutions (PAPD), by the Postgraduate Research & Practice Innovation Program of Jiangsu Province (KYCX18_1478), by the Postgraduate International Exchanges and Cooperation Project of Nanjing Medical University (C090), and the China Scholarship Council (201808320318).

Footnote

Conflicts of Interest: The authors have no conflicts of interest to declare.

Ethical Statement: All experiments were approved by the Live Animals Committee in Teaching and Research at Nanjing Medical University (Approval ID: IACUC-1703039). The study was performed in accordance with the guidelines and principles for the care and use of laboratory animals published by the National Institutes of Health (No. 85-23, revised 1996).

References

1. McCarroll CS, He W, Foote K, Bradley A, Mcglynn K, Vidler F, Nixon C, Nather K, Fattah C, Riddell A, Bowman P, Elliott EB, Bell M, Hawksby C, MacKenzie SM, Morrison LJ, Terry A, Blyth K, Smith GL, McBride MW, Kubin T, Braun T, Nicklin SA, Cameron ER, Loughrey CM. Runx1 Deficiency Protects Against Adverse Cardiac Remodeling After Myocardial Infarction. Circulation 2018;137:57-70.
2. Qian LJ, Gao Y, Zhang YM, Chu M, Yao J, Xu D. Therapeutic efficacy and safety of PCSK9-monoclonal antibodies on familial hypercholesterolemia and statin-intolerant patients: A meta-analysis of 15 randomized controlled trials. Sci Rep 2017;7:238-48.
3. Milojevic M, Head SJ, Parasca CA, Serruys PW, Mohr FW, Morice MC, Mack MJ, Ståhle E, Feldman TE, Dawkins KD, Colombo A, Kappetein AP, Holmes DR Jr. Causes of Death Following PCI Versus CABG in Complex CAD: 5-Year Follow-Up of SYNTAX. J Am Coll Cardiol 2016;67:42-55.
4. Babür Güler G, Karaahmet T, Tigen K. Myocardial fibrosis detected by cardiac magnetic resonance imaging in heart failure: impact on remodeling, diastolic function and BNP levels. Anadolu Kardiyol Derg 2011;11:71-76.
5. Hong J, Chu M, Qian LJ, Wang J, Guo Y, Xu D. Fibrillar Type I Collagen Enhances the Differentiation and Proliferation of Myofibroblasts by Lowering alpha2beta1 Integrin Expression in Cardiac Fibrosis. Biomed Res Int 2017;2017:1790808.
6. Kasner M, Westermann D, Steendijk P, Gaub R, Wilkenshoff U, Weitmann K, Hoffmann W, Poller W, Schultheiss HP, Pauschinger M, Tschöpe C. Utility of Doppler echocardiography and tissue Doppler imaging in the estimation of diastolic function in heart failure with normal ejection fraction: a comparative Doppler-conductance catheterization study. Circulation 2007;116:637-47.
7. Takemoto K, Hirata K, Hozumi T, Tanimoto T, Orii M, Shiono Y, Matsuo Y, Ino Y, Kitabata H, Kubo T, Tanaka A, Akasaka T. Noninvasive assessment of left ventricular end-diastolic pressure by deceleration time of early diastolic mitral annular velocity in patients with heart failure. Echocardiography 2017;34:1292-98.
8. Caivano D, Rishniw M, Birettoni F, Patata V, Giorgi ME, Porciello F. Left atrial deformation and phasic function determined by two-dimensional speckle-tracking echocardiography in dogs with myxomatous mitral valve disease. J Vet Cardiol 2018;20:102-14.
9. Cong T, Sun Y, Shang Z, Wang K, Su D, Zhong L, Zhang S, Yang Y. Prognostic Value of Speckle Tracking Echocardiography in Patients with ST-Elevation Myocardial Infarction Treated with Late Percutaneous Intervention. Echocardiography 2015;32:1384-91.
10. Amundsen BH, Helle-Valle T, Edvardsen T, Torp H, Crosby J, Lyseggen E, Støylen A, Ihlen H, Lima JA, Smiseth OA, Slørdahl SA. Noninvasive myocardial strain measurement by speckle tracking echocardiography:

© Quantitative Imaging in Medicine and Surgery. All rights reserved.

validation against sonomicrometry and tagged magnetic resonance imaging. J Am Coll Cardiol 2006;47:789-93.
11. Schneider M, Kostin S, Strøm CC, Aplin M, Lyngbaek S, Theilade J, Grigorian M, Andersen CB, Lukanidin E, Lerche Hansen J, Sheikh SP. S100A4 is upregulated in injured myocardium and promotes growth and survival of cardiac myocytes. Cardiovasc Res 2007;75:40-50.
12. Donato R, Cannon BR, Sorci G, Riuzzi F, Hsu K, Weber DJ, Geczy CL. Functions of S100 Proteins. Curr Mol Med 2013;13:24-57.
13. Diederichs S, Bulk E, Steffen B, Ji P, Tickenbrock L, Lang K, Zänker KS, Metzger R, Schneider PM, Gerke V, Thomas M, Berdel WE, Serve H, Müller-Tidow C. S100 family members and trypsinogens are predictors of distant metastasis and survival in early-stage non-small cell lung cancer. Cancer Res 2004;64:5564-9.
14. Wang X, Zhu Y, Sun C, Wang T, Shen Y, Cai W, Sun J, Chi L, Wang H, Song N, Niu C, Shen J, Cong W, Zhu Z, Xuan Y, Li X, Jin L. Feedback Activation of Basic Fibroblast Growth Factor Signaling via the Wnt/beta-Catenin Pathway in Skin Fibroblasts. Front Pharmacol 2017;8:32.
15. Rudolf A, Schirwis E, Giordani L, Parisi A, Lepper C, Taketo MM, Le Grand F. beta-Catenin Activation in Muscle Progenitor Cells Regulates Tissue Repair. Cell Rep 2016;15:1277-90.
16. Gatcliffe TA, Monk BJ, Planutis K, Holcombe RF. Wnt signaling in ovarian tumorigenesis. Int J Gynecol Cancer 2008;18:954-62.
17. van Noort M, Meeldijk J, van der Zee R, Destree O, Clevers H. Wnt signaling controls the phosphorylation status of beta-catenin. J Biol Chem 2002;277:17901-5.
18. Biswas M, Sudhakar S, Nanda NC, Buckberg G, Pradhan M, Roomi AU, Gorissen W, Houle H. Two- and three-dimensional speckle tracking echocardiography: clinical applications and future directions. Echocardiography 2013;30:88-105.
19. Ashraf M, Packwood WH, Zhu MH, Nickerson A, Streiff C, Sahn DJ. Evaluation of a New Strain Analysis Program Developed for Small Animal Imaging: Validation Against Sonomicrometry. Circulation 2012;126:A13223.
20. Streiff C, Panosian J, Zhu MH, Ashraf M, Sahn DJ. A Validation of Circumferential and Longitudinal Regional Strain in Pumped Hearts Modeling Normal Function Compared to Simulated Myocardial Infarction Generated From Three-Dimensional Echocardiographic Feature Tracking Compared to Sonomicrometry. Circulation 2011;124:A10677.
21. Bhan A, Sirker A, Zhang J, Protti A, Catibog N, Driver W, Botnar R, Monaghan MJ, Shah AM. High-frequency speckle tracking echocardiography in the assessment of left ventricular function and remodeling after murine myocardial infarction. Am J Physiol Heart Circ Physiol 2014;306:H1371-83.
22. Li Y, Garson CD, Xu Y, Beyers RJ, Epstein FH, French BA, Hossack JA. Quantification and MRI validation of regional contractile dysfunction in mice post myocardial infarction using high resolution ultrasound. Ultrasound Med Biol 2007;33:894-904.
23. Li Y, Garson CD, Xu Y, French BA, Hossack JA. High frequency ultrasound imaging detects cardiac dyssynchrony in noninfarcted regions of the murine left ventricle late after reperfused myocardial infarction. Ultrasound Med Biol 2008;34:1063-75.
24. Szymczyk E, Lipiec P, Plewka M, Białas M, Olszewska M, Rozwadowska N, Kamiński K, Kurpisz M, Michalski B, Kasprzak JD. Feasibility of strain and strain rate evaluation by two-dimensional speckle tracking in murine model of myocardial infarction: comparison with tissue Doppler echocardiography. J Cardiovasc Med (Hagerstown) 2013;14:136-43.
25. Qian L, Hong J, Zhang Y, Zhu M, Wang X, Zhang Y, Chu M, Yao J, Xu D. Downregulation of S100A4 alleviates cardiac fibrosis via Wnt/β–catenin pathway in mice. Cell Physiol Biochem 2018;46:2551-60.
26. Qian L, Thapa B, Hong J, Zhang Y, Zhu M, Chu M, Yao J, Xu D. The present and future role of ultrasound targeted microbubble destruction in preclinical studies of cardiac gene therapy. J Thorac Dis 2018;10:1099-111.

Cite this article as: Qian L, Zhang Y, Zhu M, Xie F, Porter TR, Xu D. Improvements in left ventricular regional and global systolic function following treatment with S100A4-shRNA after myocardial infarction in mice. Quant Imaging Med Surg 2019;9(6):1066-1075. doi: 10.21037/qims.2019.05.25

© Quantitative Imaging in Medicine and Surgery. All rights reserved.